

On special rank-two mixtures: how the zero-polytope makes life more easy

Andreas Osterloh

*Institut für Theoretische Physik, Universität Duisburg-Essen, D-47048 Duisburg, Germany.**

In the recent contribution a rather simple example of a rank-two density matrix has posed a problem in calculating upper bounds of the convex roof of the three-tangle from the zero polytope. Here, I show how a three-dimensional view, namely in terms of the Bloch-sphere analogy, solves the problem immediately. I therefore calculate the zero-polytope of the three-tangle numerically exactly (up to computer accuracy) and upper bounds to its convex roof. This method can then be applied to the more general case under consideration. Here, I apply this procedure to a superposition of the four qubit GHZ- and W-state.

I. INTRODUCTION

The entanglement content of a mixed state is represented by the convex-roof expression of the entanglement measure of interest. Whereas it is more easy to write it down than to really calculate it, it has shown to be an exactly solvable task for measures, which are SL-invariant homogeneous polynomials of rank two, as the concurrence[1, 2], respectively convex functions of them. In this simple case, the optimal decomposition has a continuous degeneracy, which is a key ingredient to the exact solution. However, already if the homogeneous degree is four, this degeneracy is lost in general and one is left with a unique solution in terms of normalized states, not considering global phases and permutations of the states. It has therefore become one of the central problems in modern physics to 'tame' the convex-roof[3]. First steps into this direction have been done in Refs. [4–6] for rank two density matrices with some thoughts about the more general case[6]. With this solution, certain particular cases for rank three density matrices[7] and even higher rank[8], all constructions out of separable states, became also possible. The convexified minimal *characteristic curve* [4–6] of the entanglement measure under consideration is the lower bound to any possible decomposition of ρ and has hence be used as lower bound to the three-tangle of general rank density matrices[9–11], a lower bound which was shown to be sharp for the class of states with the symmetry of the GHZ-state, termed *GHZ-symmetry*. This method was used later on qutrit states to demonstrate bound entanglement with positive partial transpose[12].

In the meantime several algorithms providing with upper bounds emerged[13–15], where Ref. [15] is departing from the solution for rank-two density matrices. However, also applications of the method provided in [4–6] are still challenging[16, 17]. In their recent paper [17] Jung and Park encounter a more regular case where no zeros of the three-tangle coincide. Hence, they have four single zeros for a degree-4 homogeneous polynomial invariant. Only two of them have coinciding absolute value. They

struggle with non-coinciding zeros of the characteristic curves. In the appendix of that work they give a toy-example where the very same phenomenon occurs. We first focus on their toy-example since it shows 1) how using $C_3 := \sqrt{|\tau_3|}$ instead of $|\tau_3|$ can help in calculating upper bounds of its convex-roof, and 2) the impact of not coinciding roots onto the three-tangle of the state under consideration. The intervals where the mixed three-tangle is zero can be obtained in a simple geometrical way and are numerically exact results.

This work is outlined as follows: in the next section I briefly focus on the method and give as an example the three-tangle as SL-invariant homogeneous polynomial of degree 4 with reference to [17]; the same line of thoughts can be applied however to higher degree polynomials and arbitrary rank[15], and in principle also to arbitrary invariant polynomials which are only SU-invariant with bidegree (d_1, d_2) [18, 19]. Next, I apply this method to the toy states of Ref. [17] in section III and come to some general states in section IV. I briefly comment on extended monogamy relations in section V before making concluding remarks in section VI.

II. PRELIMINARIES

For rank two density matrices ρ , the states in the range of ρ can be written as

$$|\psi(z)\rangle := |\psi_1\rangle + z|\psi_2\rangle, \quad (1)$$

with eigenstates $|\psi_i\rangle$ of ρ , and $z \in \mathbb{C}$ [6]. An entanglement measure τ vanishes precisely on the polytope with the states $|\psi(z_0)\rangle$ as vertices, where $z_0 \in \mathbb{C}$ satisfies the equation $\tau(\psi(z_0)) = 0$; this object is called the *zero-polytope*[4, 6] (see also Ref. [16]); I give an example for a polynomial of (homogeneous) degree four on the Bloch sphere in Fig. II. For density matrices of higher rank R , the states in the range of ρ can be written as

$$|\psi(z_1, \dots, z_{R-1})\rangle := |\psi_1\rangle + z_1|\psi_2\rangle + \dots + z_{R-1}|\psi_R\rangle, \quad (2)$$

and the zero-polytope turns into the convexification of the *zero-manifold* made out of all the solutions of $\tau(\psi(z_{0,1}, \dots, z_{0,R-1})) = 0$.

*Electronic address: andreas.osterloh@uni-due.de

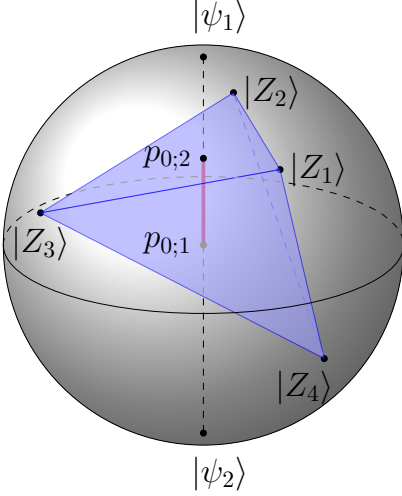


FIG. 1: An example for a (homogeneous) polynomial SL-invariant τ for a density matrix of rank two, $\rho(p) = p|\psi_1\rangle\langle\psi_1| + (1-p)|\psi_2\rangle\langle\psi_2|$ is drawn in the Bloch sphere picture. The polynomial invariant has the four solutions $|Z_i\rangle$ for $i \in \{1, \dots, 4\}$ defining the zero-polytope. The intersection of this polytope with the line connecting $|\psi_1\rangle$ and $|\psi_2\rangle$ leads to an interval $[p_{0;1}, p_{0;2}]$ of vanishing $\tau[\rho(p)]$. When this intersection is empty, this means that $\rho(p)$ is always entangled as measured by τ .

I will consider $C_3 := \sqrt{|\tau_3|}$ as entanglement measures, where the threethangle $|\tau_3|$ has been defined as[20] (see also in Refs. [21–23])

$$\begin{aligned} \tau_3 &= d_1 - 2d_2 + 4d_3 \\ d_1 &= \psi_{000}^2\psi_{111}^2 + \psi_{001}^2\psi_{110}^2 + \psi_{010}^2\psi_{101}^2 + \psi_{100}^2\psi_{011}^2 \\ d_2 &= \psi_{000}\psi_{111}\psi_{011}\psi_{100} + \psi_{000}\psi_{111}\psi_{101}\psi_{010} \\ &\quad + \psi_{000}\psi_{111}\psi_{110}\psi_{001} + \psi_{011}\psi_{100}\psi_{101}\psi_{010} \\ &\quad + \psi_{011}\psi_{100}\psi_{110}\psi_{001} + \psi_{101}\psi_{010}\psi_{110}\psi_{001} \\ d_3 &= \psi_{000}\psi_{110}\psi_{101}\psi_{011} + \psi_{111}\psi_{001}\psi_{010}\psi_{100} \end{aligned}$$

and coincides with the three-qubit hyperdeterminant[24, 25]. It is the only continuous SL-invariant, meaning that every other such SL-invariant for three qubits can be expressed as a function of τ_3 .

III. THE TOY EXAMPLE RAISED BY JUNG AND PARK

We define the n -qubit GHZ- and W-states as

$$|GHZ_n\rangle = \frac{1}{\sqrt{2}}(|00\dots 0\rangle + |11\dots 1\rangle) \quad (3)$$

$$\begin{aligned} |W_n\rangle &= \frac{1}{\sqrt{3}}(|0\dots 01\rangle + |0\dots 10\rangle + \dots \\ &\quad + |10\dots 0\rangle) \end{aligned} \quad (4)$$

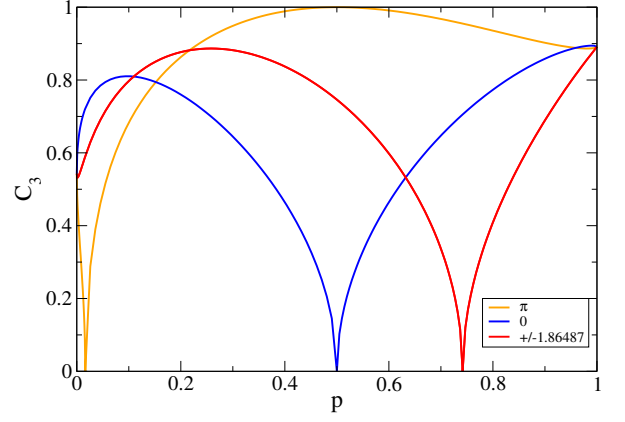


FIG. 2: The four characteristic curves for C_3 whose three-angle becomes zero are shown: two single real zeros at $p \approx 0.01636$ (orange curve) and $p = 0.5$ (purple curve) corresponding to an angle $\varphi = \pi$ and $\varphi = 0$, respectively, and the two coinciding curves which are zero at $p \approx 0.7418$ (red curve). The latest curve corresponds to two complex conjugate solutions z_0 . Both curves are for the angle $\varphi = \pm 1.8649 = \arg(z_0)$. The angles of z for the different curves are shown in the legend.

where we consider the three-qubit example first

$$|GHZ_3\rangle = \frac{1}{\sqrt{2}}(|000\rangle + |111\rangle) \quad (5)$$

$$|W_3\rangle = \frac{1}{\sqrt{3}}(|001\rangle + |010\rangle + |100\rangle) \quad (6)$$

and the density matrix

$$\rho(p) = p|\psi_1\rangle\langle\psi_1| + (1-p)|\psi_2\rangle\langle\psi_2|, \quad (7)$$

where

$$|\psi_{\pm}\rangle = \frac{1}{\sqrt{2}}(|GHZ_3\rangle \pm |W_3\rangle). \quad (8)$$

These states satisfy the orthogonality condition $\langle\psi_+|\psi_- \rangle = 0$. In order to calculate or estimate the three-angle in $\rho(p)$, we have to consider the characteristic curves[4, 6], hence

$$C_3(p, \varphi) := C_3(Z(p, \varphi)) \quad (9)$$

for the states

$$|Z(p, \varphi)\rangle := \sqrt{p}|\psi_+\rangle - e^{i\varphi}\sqrt{1-p}|\psi_-\rangle. \quad (10)$$

Some of them are shown in Fig. 2 (more can be found in Ref. [17]). It is hence useful to look for solutions z_0 to the equation

$$\tau_3(|\psi_+\rangle - z|\psi_-\rangle) = 0. \quad (11)$$

The zeros $z_{0;j}$, $j = 1, \dots, 2n$ with $n \in \mathbf{N}$, describe the vertices of a zero-polytope, which becomes a three dimensional zero-simplex in this case. I want to emphasize that the zero-simplex is an exact result and therefore the

values p of $\rho(p)$ which are lying inside the zero simplex are the only values for which the convex roof of $\rho(p)$ vanishes. Hence, it is also clear that the complement is made out of states with non-zero convex-roof. The zeros of Eq. 11 are

$$\mathbf{z}_0 = (z_{0;1}, z_{0;2}, z_{0;3}, z_{0;4}) \quad (12)$$

$$\approx (1, -7.7543, 0.5899e^{1.8649i}, 0.5899e^{-1.8649i}) \quad (13)$$

I want to emphasize that although the values for the zeros are exact, they are nevertheless approximated here since it is cumbersome to write them down analytically; in addition, I don't attribute to the knowledge of the exact values any further insight. With $p_0 = p(z_0) = 1/(1 + |z_0|^2)$, hence

$$\begin{aligned} \mathbf{p}_0 &= (p_{0;1}, p_{0;2}, p_{0;3}, p_{0;4}) \\ &\approx (1/2, 0.01636, 0.74182, 0.74182), \end{aligned} \quad (14)$$

the values $p_0 z_0$ are those to be convexly combined to zero[15, 16]. The result is that for $p \in [0.11423, 0.69289]$ the convex roof of the three-tangle is zero. The decomposition of $\rho(p)$ in $p = 0.11423$ is given by $|Z(p_{0;1}, 0)\rangle$ with weight 0.202362 and $|Z(p_{0;2}, \pi)\rangle$ with weight 0.797638; at $p = 0.692885$ it is given by $|Z(p_{0;1}, 0)\rangle$ with weight 0.202362 and the states $|Z(p_{0;3} = p_{0;4}, \pm 1.86487)\rangle$ with weights 0.398819 each. It is a curious coincidence that the weight of $|Z(p_{0;1}, 0)\rangle$ takes the same value; they deviate only by 3×10^{-16} .

An upper bound to the convex-roof \widehat{C}_3 is shown in Fig. 3 together with the characteristic (gray background) curves: the upper bound to the convex-roof is a piecewise straight (orange) line. I will therefore call it the *linearized* upper bound. The strong concavity of the characteristic curves around their zeros, together with the fact that the plotted characteristic curves close to their zeros are a lower bound to other characteristic curves, tells that whatever decomposition vector of the density matrix one will take it will yield in a concave result at least in the vicinity of the zero-simplex. This modifies close to $p = 0$ or $p = 1$ where it is rather likely that a piecewise convex curve might be obtained, in particular in the interval $[0, 0.11423]$ where one of the characteristic curves is strongly convexly decreasing with a zero at $p \approx 0.01636$. I therefore try for a slightly different decomposition here in order to check whether the convexity of this characteristic curve might lead to a curve which somewhere lies below the straight line. I chose to decompose the matrix $\rho(p)$ into two states, namely into the state $|Z(p_{0;1}, 0)\rangle$ and the corresponding state $|Z(q(p, p_{0;1}), \pi)\rangle$ with $q(p, p_{0;1})$ in the interval given by p and $p_{0;1}$ such that the line connecting the states $|Z(p_{0;1}, 0)\rangle$ and $|Z(q(p, p_{0;1}), \pi)\rangle$ on the Bloch sphere hits the point on the z-axis corresponding to $\rho(p)$. A further decomposition I had a look at, is the equal mixture of the two states $|Z(p_{0;3} = p_{0;4}, \pm 1.86487)\rangle$ with $|Z(q(p, p_{0;1}), 0)\rangle$ such that the line interconnecting the two states is again passing $\rho(p)$. The result is shown as red dashed lines in Fig. 4. Some

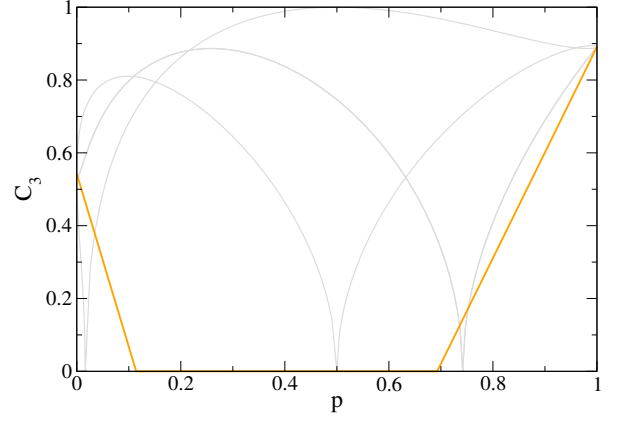


FIG. 3: An upper bound to the convex-roof is shown for $\rho(p)$ (orange line). It is piecewise linearly interpolating between $(p, C_3) = (0, \sqrt{8\sqrt{6}-9}/6)$, $(0.11423, 0)$, $(0.69289, 0)$, and $(1, \sqrt{8\sqrt{6}+9}/6)$. The intersection of $\rho(p)$ with the zero-simplex of the three-tangle is an exact result, whereas the linear extrapolation is certainly an upper bound to $C_3 = |\sqrt{\tau_3}|$; it results from a superposition of the corresponding pure state and the density matrix with zero three-tangle closest to it. Therefore the density matrix would be decomposed into three states for $0 < p < 0.11423$ and into four states for $0.692885 < p < 1$. The characteristic curves are the gray curves in the background; they serve in order to demonstrate how the intersection with the zero-simplex, due to its convexity, leads to a shrinking of the region where $C_3[\rho(p)] = 0$.

of them are lying below the straight line, demonstrating that a better upper bound than the linearized one is obtained for the convex-roof \widehat{C}_3 . It is linear close to the borders of the interval $[0.11423, 0.692885]$ up to $p_r = 0.8240$ and down to $p_l = 0.04395$, showing that the decomposition is made of convex decompositions of the two states $|Z(p_{0;3} = p_{0;4}, \pm 1.86487)\rangle$ and a third state $|Z(q(p_l/r, p_{0;1}), 0)\rangle$ (see Refs. [4, 6]). Beyond it is strictly convex, telling that the decomposition is here made of the two states $|Z(p_{0;3} = p_{0;4}, \pm 1.86487)\rangle$ and the state $|Z(q(p, p_{0;1}), 0)\rangle$, which depends on p .

This procedure will be repeated for the general rank-two case in the next section. It can be applied for general rank-two density matrices and, using the results of Ref. [15], also for obtaining useful upper bounds for general rank. It is a purely geometric method and therefore it is not restricted to qubits.

IV. THE INTERESTING CASE

We now turn to the more general example where the pure state

$$|\Psi_4(p, \varphi)\rangle := \sqrt{p} |GHZ_4\rangle - \sqrt{1-p} e^{i\varphi} |W_4\rangle \quad (15)$$

of four-qubits was given[17]. It is a permutation invariant state whose three-qubit density matrices, for their

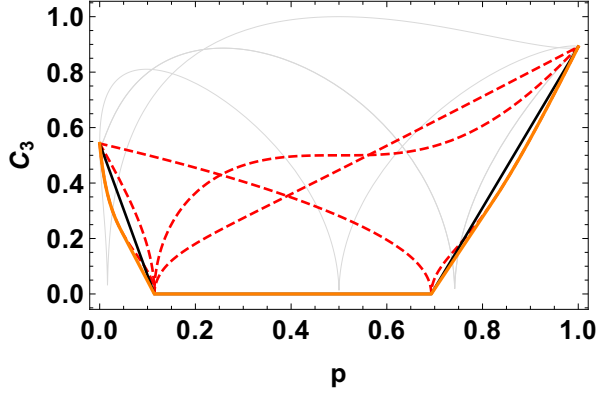


FIG. 4: Here, I show results for some particular decompositions of $\rho(p)$ (read the text for details). The characteristic curve with a single zero at $p = 0.01636$, corresponding to an angle $\varphi = \pi$, initially is strictly convex. Therefore that decompositions containing a state $|Z(q, \pi)\rangle$ will be also strictly convex close to the points $p = 0, 1$. That this is indeed the case also for p close to 1 is shown by the red dashed curves, which comes to lie below the upper linearized bound (thin black line). The corresponding new lower bound is the thick orange line.

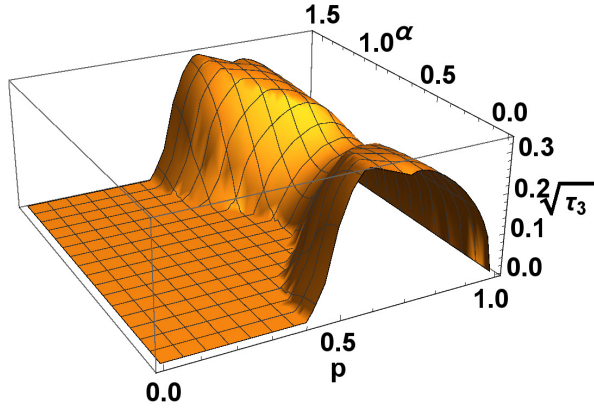


FIG. 5: The upper bound for \widehat{C}_3 where one linearizes between the values for the states $|\psi_i(p, \varphi)\rangle$ and the corresponding extreme intersection points $p_{0,i}$, for $i = 1, 2$, of the line represented by $\rho(p)$ and the zero-simplex.

permutational symmetrie, all have the same form

$$\rho_3(p, \varphi) = q(p)|\psi_1(p, \varphi)\rangle\langle\psi_1(p, \varphi)| + (1 - q(p))|\psi_2(p, \varphi)\rangle\langle\psi_2(p, \varphi)| \quad (16)$$

with $q(p) = \frac{2 + \sqrt{1 - p^2}}{4}$ and

$$\psi_1(p, \varphi) = f_1(p)e^{i\varphi}|111\rangle + g_1(p)|000\rangle + h_1(p)e^{-i\varphi}|W_3\rangle \quad (17)$$

$$\psi_2(p, \varphi) = f_2(p)e^{i\varphi}|111\rangle + g_2(p)|000\rangle + h_2(p)e^{-i\varphi}|W_3\rangle. \quad (18)$$

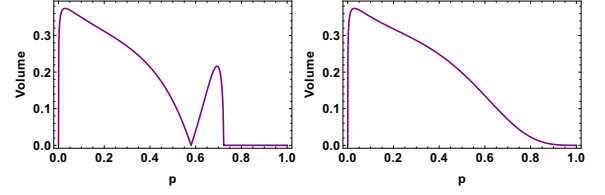


FIG. 6: The volume of the zero-simplex for two values of $\varphi = 0$ and $\varphi = \pi/4$. For $\varphi = 0$ the volume grows to a finite value for diminishing again unless it is crossing with zero volume (staying however two-dimensional) to grow again up to a value of $p = 0.722074$ where it again becomes two-dimensional up to $p = 1$. Here, the imaginary part of the two corresponding solutions is zero and we have again four real values. This passage through zero in between is missing for $\varphi = \pi/4$; in particular the zero-simplex is always three-dimensional for $p \in (0, 1)$.

Here, the functions are defined as

$$f_1(p) := \sqrt{\frac{2}{(1+p)(3-p) + (3+p)\sqrt{1-p^2}}} p \quad (19)$$

$$g_1(p) := \sqrt{p \frac{4\sqrt{1-p^2} - 3p + 5}{(3+p)\sqrt{1-p^2} + (1+p)(3-p)}} \quad (20)$$

$$h_1(p) := \sqrt{\frac{3p(1-p)}{(1+p)^2 - (1-p)\sqrt{1-p^2}}} \quad (21)$$

$$f_2(p) := \sqrt{\frac{2}{(1+p)(3-p) - (3+p)\sqrt{1-p^2}}} p \quad (22)$$

$$g_2(p) := \sqrt{p \frac{4\sqrt{1-p^2} + 3p - 5}{(3+p)\sqrt{1-p^2} - (1+p)(3-p)}} \quad (23)$$

$$h_2(p) := \sqrt{-\frac{3p(1-p)}{(1+p)^2 + (1-p)\sqrt{1-p^2}}}. \quad (24)$$

The three-tangle is a periodic function of φ with period $\pi/2$, because of a four qubit symmetric state. We show the results of the algorithm from Ref. [15], which except the default linearization is an exact result for the zeros, in Fig. 5. It is an upper bound to \widehat{C}_3 .

In order to test whether it is possible also here to come below the linearized upper bound, I checked the zeros of Eq. 11 and the particular decompositions I have described in detail in the last section.

In $[0.722074, 1]$, there are 4 real solutions. For the remaining values of p , there are two complex conjugate solutions besides the two which stay real. One decomposition for which the three-tangle vanishes is always made from real solutions here, whereas the other one is made out of three pure states: one corresponding to a real solution and the two complex conjugate solutions. The zero-simplex is varying its dimension as shown in Fig. 6 for $\varphi = 0$ and $\varphi = \pi/4$ respectively. It is becoming zero twice for $\varphi = 0$: a single point, where the line spanned

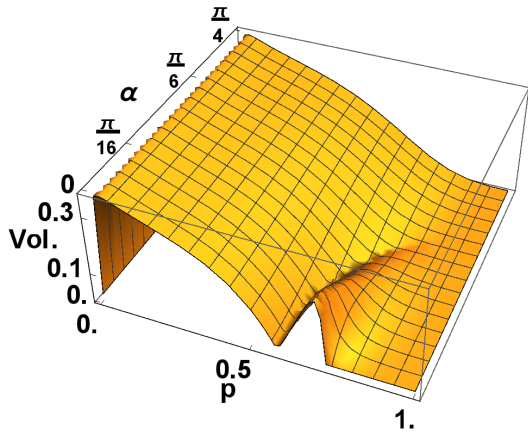


FIG. 7: A three-dimensional plot of the zero-simplex dimension.

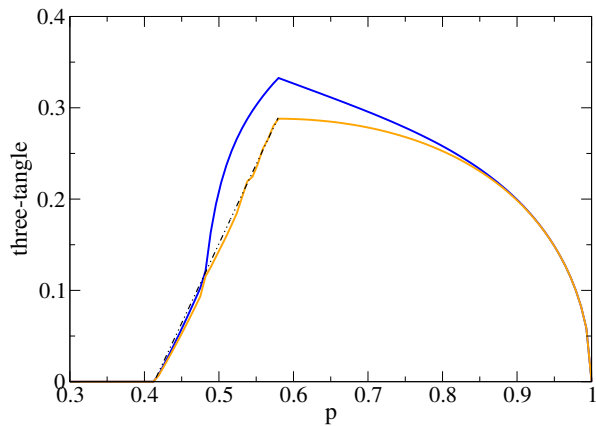


FIG. 8: Two upper bounds for \widehat{C}_3 for $\varphi = 0$ as a function of p . Besides the linearized version from Ref. [15] (upper blue curve) also the one coming out of the procedure described here (see discussion of Fig. 4) is shown (orange lower curve). This curve is well approximated with the straight black dash-dotted line in the figure. It can be seen however that the convex-roof lies at least slightly below the straight line.

by the complex conjugate values with non-zero imaginary part crosses the corresponding line between the two other real values, and there is a whole interval $[0.722074, 1]$ for p where the zero-simplex is two-dimensional. There, four real solutions appear. This feature however is not stable against small perturbations in φ .

The single zero disappears for $\varphi \gtrsim 0.5236$ with the zero-simplex being everywhere three-dimensional (except at the boundaries); in particular for $\varphi = \pi/4$. This is indicated in Fig. 7.

The three-tangle C_3 is given for $\varphi = 0$ in the linearized version and the procedure described in section III (see also the discussion of Fig. 4 in the text). It is seen that both basically coincide close to the zeros but they deviate considerably in between. This is not the case for $\varphi = \pi/4$, where both curves coincide (not shown here).

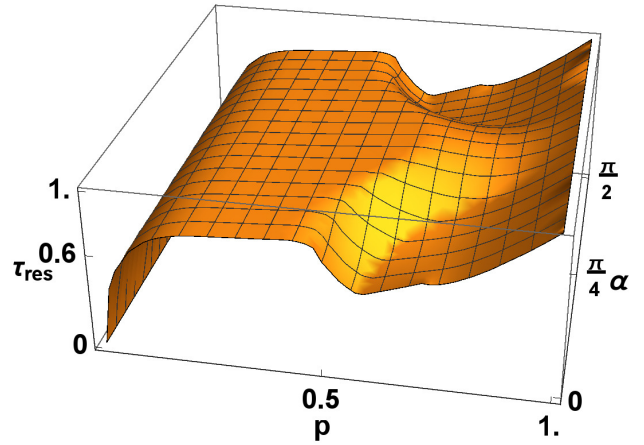


FIG. 9: The extended residual tangle[27–30] using \widehat{C}_3^2 as the measure for the three-tangle. I do not show the outcome for $\widehat{\sqrt{C_3}}^4$, since it is smaller than \widehat{C}_3^2 [16] and accordingly the residual tangle is bigger.

V. EXTENDED MONOGAMY

It is clear that the residual tangle is not measured in general by an SL-invariant quantity[26]. Therefore it makes little sense to subtract from the residual tangle which has no SL-invariance an SL-invariant quantity. When doing so instead one recognizes that the monogamy cannot be extended with the usual three-tangle $\widehat{\tau}_3$ or even its square root $\widehat{\sqrt{\tau_3}}^2 = \widehat{C}_3^2$ [27–29]. The ultimate possibility would be $\widehat{\sqrt[4]{\tau_3}}^4$, which could not be excluded for pure states of four qubits[30]. This doesn't mean that it won't be excluded for some n -qubit pure state with $n > 4$. This question has to be answered in future work. As far as the extended monogamy relations are concerned, the states already satisfy it taking \widehat{C}_3^2 as measure for the three-tangle. This can be seen in Fig. 9 taking the linearized upper bound for \widehat{C}_3^2 ; it therefore provides a lower bound for the residual tangle. It is ranging from zero (for the W-states) to one (for the GHZ-states).

VI. CONCLUSIONS

In a recent contribution, Jung and Park have tempted to test the monogamy relations of Coffman, Kundu and Wootters (CKW)[20] and for the negativity[31, 32] towards possible extended versions[27–29, 33]. They succeeded for the negativity, however they encountered problems for the Coffman-Kundu-Wootters-monogamy, which they highlighted using a toy-example in their appendix. I have described in detail for this toy example of Ref. [17] how the zeros of the convex-roof can be determined exactly (up to the corresponding computer accuracy), how

the simplest linearized version of an upper bound can be obtained, and how one can go beyond it. Therefore, I calculate the upper bound of the three-tangle $\sqrt{\tau_3}$ for the toy model. I apply this formalism to the general case of superpositions of four-particle GHZ and W states, calculating the linearized form for the upper bound together with the extended version for $\sqrt{\tau_3}$. I want to mention that the calculation of the three-tangle of $\rho = p|GHZ_4\rangle\langle GHZ_4| + (1-p)|W_4\rangle\langle W_4|$ is trivial since it is equal to zero for each three-qubit subsystem. Then

I briefly comment on the extended CKW-monogamy and provide a graph also here.

Acknowledgements

I acknowledge discussions with K. Krutitsky and R. Schützhold.

-
- [1] W. K. Wootters, Phys. Rev. Lett. **80**, 2245 (1998).
 - [2] A. Uhlmann, Phys. Rev. A **62**, 032307 (2000).
 - [3] B. Jungnitsch, T. Moroder, and O. Gühne, Phys. Rev. Lett. **106**, 190502 (2011).
 - [4] R. Lohmayer, A. Osterloh, J. Siewert, and A. Uhlmann, Phys. Rev. Lett. **97**, 260502 (2006).
 - [5] C. Eltschka, A. Osterloh, J. Siewert, and A. Uhlmann, New J. Phys. **10**, 043014 (2008).
 - [6] A. Osterloh, J. Siewert, and A. Uhlmann, Phys. Rev. A **77**, 032310 (2008).
 - [7] E. Jung, M.-R. Hwang, D. Park, and J.-W. Son, Phys. Rev. A **79**, 024306 (2009).
 - [8] H. Shu-Juan, W. Xiao-Hong, F. Shao-Ming, S. Hong-Xiang, and W. Qiao-Yan, Comm. Theor. Phys. **55**, 251 (2011).
 - [9] C. Eltschka and J. Siewert, Phys. Rev. Lett. **108**, 020502 (2012).
 - [10] J. Siewert and C. Eltschka, Phys. Rev. Lett. **108**, 230502 (2012).
 - [11] C. Eltschka and J. Siewert, Phys. Rev. A **89**, 022312 (2014).
 - [12] G. Sentís, C. Eltschka, and J. Siewert, pra **94**, 020302(R) (2016).
 - [13] K. Cao, Z.-W. Zhou, G.-C. Guo, and L. He, Phys. Rev. A **81**, 034302 (2010).
 - [14] S. Rodrigues, N. Datta, and P. Love, Phys. Rev. A **90**, 012340 (2014).
 - [15] A. Osterloh, Phys. Rev. A **93**, 052322 (2016).
 - [16] A. Osterloh, Phys. Rev. A **94**, 012323 (2016).
 - [17] E. Jung and D. Park (2016), arXiv:1607.00135.
 - [18] J.-G. Luque, J.-Y. Thibon, and F. Toumazet, Math. Struct. Comp. Sc. **1133** (2007).
 - [19] M. Johansson, M. Ericsson, E. Sjöqvist, and A. Osterloh, Phys. Rev. A **89**, 012320 (2014).
 - [20] V. Coffman, J. Kundu, and W. K. Wootters, Phys. Rev. A **61**, 052306 (2000).
 - [21] A. Wong and N. Christensen, Phys. Rev. A **63**, 044301 (2001).
 - [22] F. Verstraete, J. Dehaene, and B. De Moor, Phys. Rev. A **68**, 012103 (2003).
 - [23] A. Osterloh and J. Siewert, Phys. Rev. A **72**, 012337 (2005).
 - [24] A. Cayley, Journal für reine und angewandte Mathematik **30**, 1 (1846).
 - [25] A. Miyake and M. Wadati, Quant. Info. Comp. **2**, 540 (2002).
 - [26] C. Eltschka, A. Osterloh, and J. Siewert, Phys. Rev. A **80**, 032313 (2009).
 - [27] B. Regula, S. D. Martino, S. Lee, and G. Adesso, Phys. Rev. Lett. **113**, 110501 (2014).
 - [28] B. Regula, S. D. Martino, S. Lee, and G. Adesso, Phys. Rev. Lett. **116**, 049902 (2016), erratum.
 - [29] B. Regula and G. Adesso, Phys. Rev. Lett. **116**, 070504 (2016).
 - [30] B. Regula, A. Osterloh, and G. Adesso (2016), arXiv:1604.03419.
 - [31] Y.-C. Ou and H. Fan, Phys. Rev. A **75**, 062308 (2007).
 - [32] H. He and G. Vidal, Phys. Rev. A **91**, 012339 (2015).
 - [33] S. Karmakar, A. Sen, A. Bhar, and D. Sarkar, Phys. Rev. A **93**, 012327 (2016).